Pull-apart basin formation and development in narrow transform zones with application to the Dead Sea Basin

Jeroen Smit, Sierd Cloetingh, Z. Ben-Avraham, Jean-Pierre Brun

Pull-apart basin formation and development in narrow transform zones with application to the Dead Sea Basin

J. Smit,[1,2,3] J.-P. Brun,[2] S. Cloetingh,[1] and Z. Ben-Avraham[4]

Received 20 February 2007; revised 8 September 2008; accepted 9 October 2008; published 31 December 2008.

[1] Contrary to other examples, like Death Valley, California, and the Sea of Marmara, Turkey, the Dead Sea-type pull-apart basins form within a narrow transform corridor between strike-slip faults that are less than 10 km apart, much smaller than the crustal thickness of 35 km. In this paper we investigate the role of fault zone width versus thickness and rheology on the mechanics of pull-apart basins through a series of laboratory experiments. Results show that pull-apart basins that develop above a small step over (i.e., smaller than the thickness of the brittle layer") are narrow and elongated parallel to the overall motion. This is enhanced by increased decoupling along a basal ductile layer. The experiment with the highest degree of mechanical decoupling shows a striking resemblance to the Dead Sea Basin (DSB). Comparison with modeling results suggests that the DSB's flat basin floor is bordered over its full length by strike-slip faults that control the basin geometry and temporal and spatial basin migration. This is in strong contrast to Death Valley-type pull-apart basins that are highly oblique to the transform direction with transverse normal faults dominating over longitudinal strike-slip faults. Results imply that lithosphere rheology and the ratio of basin width to crustal thickness are controlling factors in the mechanics of pull-apart basin formation within transform corridors like the Dead Sea Fault. **Citation:** Smit, J., J.-P. Brun, S. Cloetingh, and Z. Ben-Avraham (2008), Pull-apart basin formation and development in narrow transform zones with application to the Dead Sea Basin, *Tectonics*, *27*, TC6018, doi:10.1029/2007TC002119.

1. Introduction

[2] Pull-apart basins are prominent features along continental transform faults like the San Andreas Fault, Dead Sea Fault and Alpine Fault of New Zealand [e.g., *Crowell*, 1974; *Aydin and Nur*, 1982; 1985; *Ben-Avraham*, 1985; *Christie-Blick and Biddle*, 1985; *Sylvester*, 1988; *Ben-Avraham*, 1997; *ten Brink et al.*, 1999; *Garfunkel and Ben-Avraham*, 2001]. These basins are important sources of information concerning the history of the transform, recorded in their sedimentary fill.

[3] The Dead Sea Fault (DSF) displays a series of pull-apart basins that are, from south to north, the basins of the Gulf of Aqaba, the Dead Sea, the Sea of Galilee, the Hula basin, and the El Ghab basin (Figure 1). All these basins are located within the transform corridor [e.g., *Garfunkel and Ben-Avraham*, 2001] and none of them is wider than the corridor itself, except for the Sea of Galilee, whose anomalous geometry is due to the interference of the faults defining the corridor with normal faults located outside [*Hurwitz et al.*, 2002]. All other basins are elongated and parallel to the corridor borders. Their long sides are defined by strike-slip and normal faults and the short sides are flexural or defined by normal faults. The Dead Sea Basin is, with a total length of 150 km and a depth to basement of more than 8 km, among the largest and most studied pull-apart basins worldwide [e.g., *Zak and Freund*, 1981; *Kashai and Croker*, 1987; *Garfunkel and Ben-Avraham*, 1996; *Niemi et al.*, 1997; *Al-Zoubi et al.*, 2002; *Cloetingh and Ben-Avraham*, 2002; *Larsen et al.*, 2002; *Enzel et al.*, 2006]. It is composed of three narrow and elongated subbasins. The very steep subsidence gradients are accommodated along a small number of closely spaced faults.

[4] Striking differences exist between the geometries of the Dead Sea Basin and other pull-apart basin such as the Death Valley Basin [e.g., *Burchfiel and Stewart*, 1966; *Wright and Troxel*, 1999] (Figure 2). The transform-parallel orientation of the Dead Sea Basin and its elongated, nearly rectangular geometry contrasts with the highly transform-oblique Death Valley pull-apart basin. The Dead Sea subbasins are oriented in-line, while gravity analysis shows four subbasins with an en echelon orientation in the Death Valley Basin [*Blakely et al.*, 1999]. The strike-slip fault/normal (longitudinal/orthogonal) fault length ratio is around 9 in the Dead Sea Basin and 0.3 in the Death Valley Basin. The spacing between strike-slip faults is less than 10 km in the Dead Sea and almost 40 km in the Death Valley. As the two examples have a comparable crustal thickness of 35–40 km [e.g., *Ginzburg et al.*, 1981; *Ruppert et al.*, 1998; *Desert Group et al.*, 2004; *Mohsen et al.*, 2006], the ratio between the strike-slip fault spacing and crustal thickness is less than 0.25 for the Dead Sea and around 1 for the Death Valley. In the large spectrum of pull-apart basin geometries [e.g., *Crowell*, 1974; *Aydin and Nur*, 1982; 1985; *Basile and*

[1]Netherlands Research Centre for Integrated Solid Earth Sciences, Faculty of Earth and Life Sciences, Vrije Universiteit, Amsterdam, Netherlands.
[2]Géosciences Rennes, Université de Rennes 1, Rennes, France.
[3]Now at Department of Earth Sciences, ETH Zurich, Zurich, Switzerland.
[4]Department of Geophysics and Planetary Sciences, Tel Aviv University, Tel Aviv, Israel.

0278-7407/08/2007TC002119

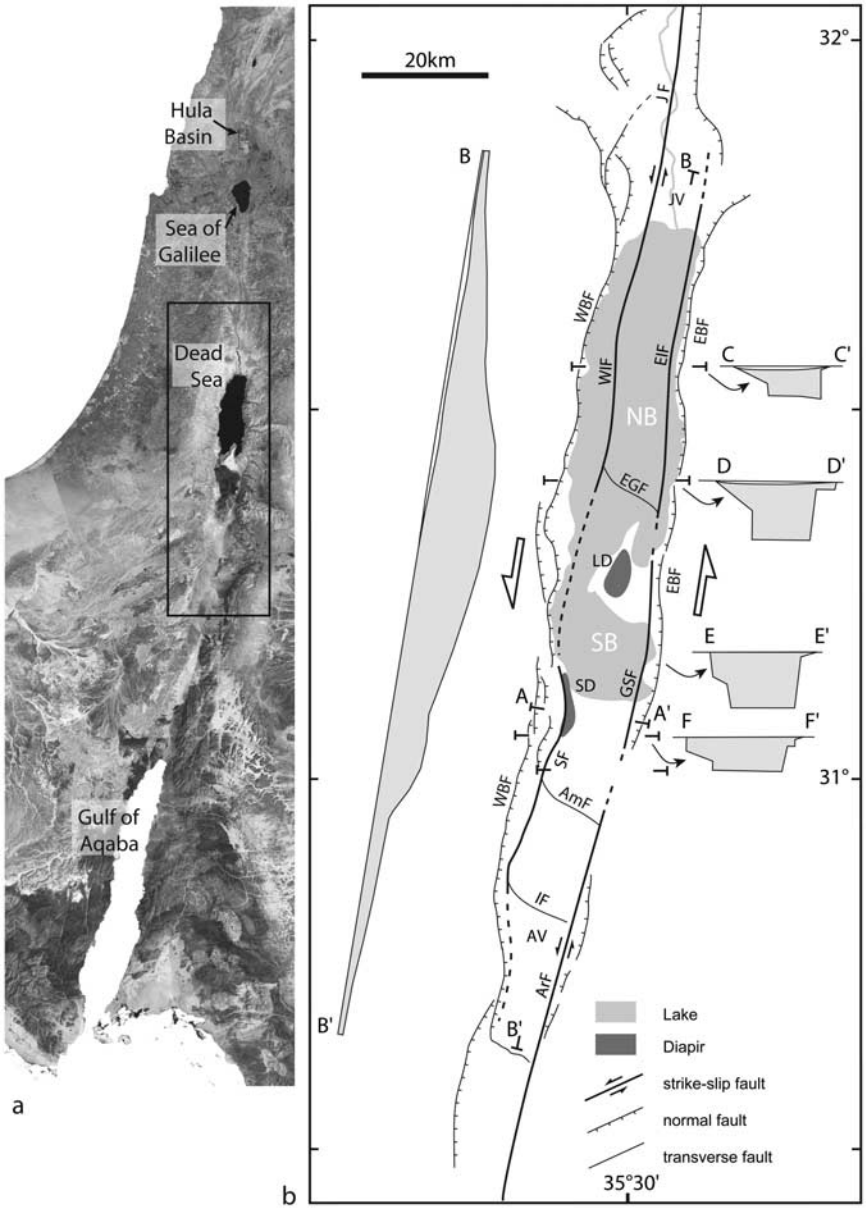

Figure 1. (a) Landsat 7 image of the Dead Sea Fault with location of the Dead Sea Basin. (b) Structural map of the Dead Sea Basin (modified from *Garfunkel and Ben-Avraham* [1996] and *Kashai and Croker* [1987]) with profiles based on gravity modeling from *ten Brink et al.* [1993]. Profile AA' is shown in Figure 3. AmF, Amazyahu Fault; ArF, Arava Fault; AV, Arava Valley; EBF, Eastern Boundary Fault; EGF, Ein Gedi Fault; EIF, Eastern Intermediate Fault; GSF, Ghor Safi Fault; IF, Iddan Fault; JF, Jericho (Jordan) Fault; JV, Jordan Valley; LD, Lisan Diapir; SD, Sedom Diapir; SF, Sedom Fault; WBF, Western Border Fault; WIF, Western Intermediate Fault.

Brun, 1999; *Wakabayashi et al.*, 2004], the above mentioned nondimensional numbers suggest that the Dead Sea and the Death Valley basins represent end-member cases.

[5] Despite the large amount of available data, fundamental questions remain on the internal geometry and the mechanisms controlling the Dead Sea Basin evolution. Of particular importance in this context is the role of strain partitioning between longitudinal faults, the role of transverse faults and the occurrence of basin migration. Since the recognition of strike-slip movement within the basin is rather difficult, the nature of individual faults is often questioned, as is the timing of movement.

[6] In the present paper, we address the influence of rheology and fault zone width versus thickness on pull-apart basin development in narrow transform zones. We present a series of laboratory experiments specifically designed to study pull-apart basin formation and development in narrow transform fault zones like the Dead Sea

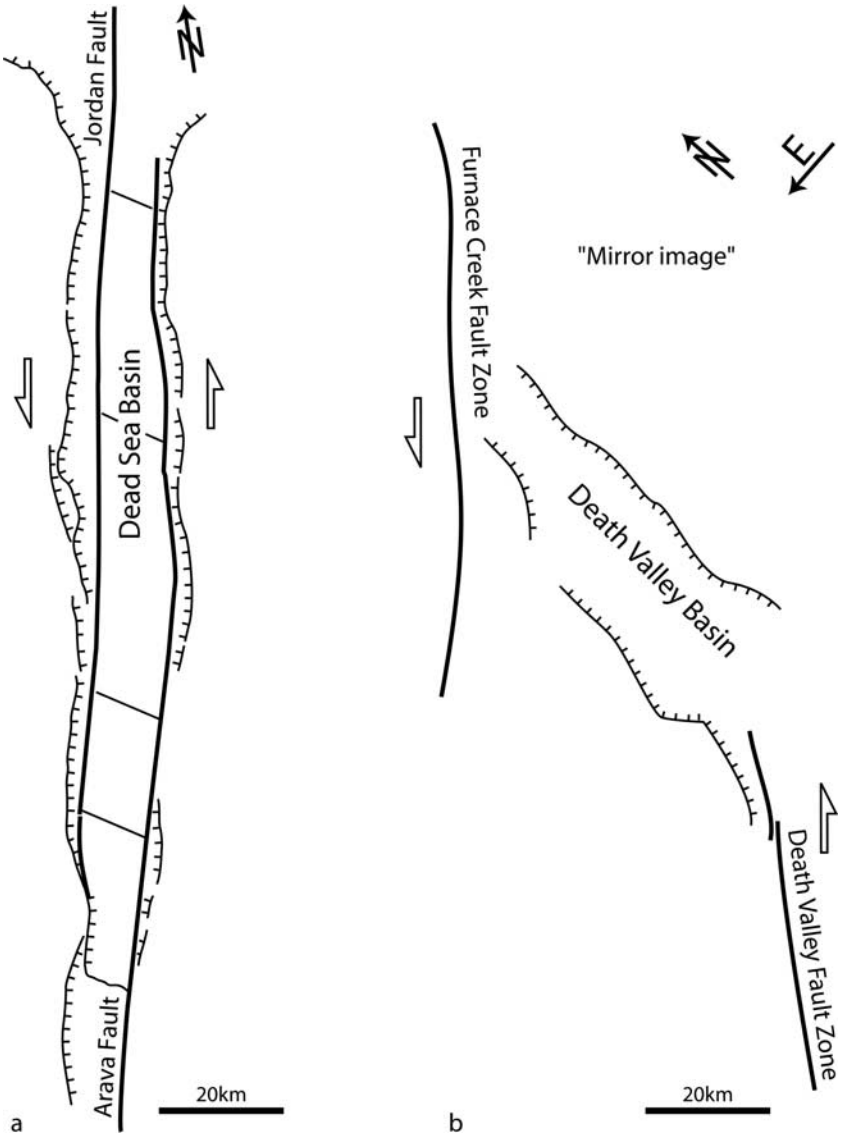

Figure 2. The remarkably different geometries of pull-apart basins of (a) the Dead Sea (modified from data of *Garfunkel and Ben-Avraham* [1996]) and (b) the Death Valley (modified from *Burchfiel and Stewart* [1966]). Spacing between strike-slip faults is less than 10 km in the Dead Sea and almost 40 km in the Death Valley. The strike-slip fault/normal fault length ratio is approximately 9 in the Dead Sea and 0.3 in the Death Valley. Figure conventions are as in Figure 1b.

Fault. The experimental results and their implications for the development of pull-apart basins in general and those in narrow fault zones in particular, are discussed after the example of Death Valley and the Dead Sea Basin.

2. Dead Sea Basin

2.1. Plate Tectonic Setting

[7] The Dead Sea Fault relates the opening of the Red Sea to the south, to the Taurus-Zagros collision to the north, with since 15 Ma an amount of about 100 km of sinistral displacement between the Arabian and African plates [e.g., *Quennell*, 1959; *McKenzie et al.*, 1970].

[8] A regional change in plate kinematics took place around 5 Ma ago, more or less coeval with the onset of oceanic accretion in the Red Sea [e.g., *Izzeldin*, 1987; *Le Pichon and Gaulier*, 1988]. In the Taurus Mountains a change from compression to strike slip was dated at around 5 Ma [e.g., *Kocyigit et al.*, 2001] marks the initiation of the east and north Anatolian faults that accommodate the westward extrusion of Anatolia [e.g., *Sengör et al.*, 1985; *Le Pichon and Gaulier*, 1988]. The more or less coeval formation of the Sea of Galilee and Hula depression together with the initiation of the main subsidence in the Dead Sea Basin and the Gulf of Aqaba is dated at around 5 Ma as well [e.g., *Garfunkel and Ben-Avraham*, 2001].

[9] The southern half of the Dead Sea Fault is bordered by steep fault scarps that have resulted in a rift valley-like morphology of 5 to 20 km wide [e.g., *Quennell*, 1958, 1959; *Wdowinski and Zilberman*, 1997]. This has been attributed to a slight component of extension in addition to the overall strike-slip movement [*Quennell*, 1958, 1959; *Wdowinski and Zilberman*, 1997], which has been related to the plate kinematics change around 5 Ma [e.g., *Garfunkel*, 1981]. The asymmetry of the DSF that appears in both cross section and plan view is marked by higher vertical fault offsets and related flank uplift and erosion along the eastern side of the rift valley [e.g., *Quennell*, 1958; *Garfunkel*, 1981; *Wdowinski and Zilberman*, 1997; *Basile and Allemand*, 2002]. A total amount of 107 km of left-lateral displacement is deduced from geological correlation, with 62 km displacement during the Miocene and 45 km since the Pliocene [*Quennell*, 1959]. Regional-scale reconstructions of plate kinematics between Eurasia, Africa and Arabia sustain an initiation of the DSF around 15 Ma and a change in the kinematics of Arabia around 5 Ma [e.g., *Joffe and Garfunkel*, 1987; *Le Pichon and Gaulier*, 1988; *Chu and Gordon*, 1998; *Bosworth et al.*, 2005]. The present displacement rate along the DSF is estimated at 4–5 cm/a based on recent GPS constraints [*Reilinger et al.*, 2006].

[10] For full reviews on geology and geophysics of the Dead Sea and its regional setting see *Niemi et al.* [1997], *Garfunkel and Ben-Avraham* [2001], *Cloetingh and Ben-Avraham* [2002] and *Enzel et al.* [2006], among others.

2.2. Basin Geometry

[11] The Dead Sea Basin (DSB) formed in the Miocene as a pull-apart basin between two en echelon strike-slip fault segments, the Jericho Fault to the west and the Arava Fault to the east (Figure 1). With a total length of more than 150 km and a width of up to 15–17 km, the DSB is among the largest pull-apart basins worldwide. The basin reaches a maximum depth of 8.5 km or more in its central part under the Lisan Diapir, as indicated by depth conversion of seismic lines [*Al-Zoubi and ten Brink*, 2001] and gravity data analyses (Figure 1b) [*ten Brink et al.*, 1993]. The Dead Sea Basin initiated to the south of the presently active basin in the Arava Valley, as demonstrated by a thick succession of Miocene lacustrine clastic sediments [e.g., *Kashai and Croker*, 1987; *Garfunkel*, 1997]. The active DSB is subdivided in a northern and a southern subbasin by the Lisan peninsula, a large salt diapir. The 45–50 km long northern subbasin is the location of the present-day Dead Sea, a 350 m deep hypersaline lake with a water level at 400 m below Mediterranean Sea Level. The subaerial central subbasin was until 50 years ago covered by the lake and therefore known as the southern Dead Sea. The difference in depth between the subaerial South basin and the 350 m deep north basin, suggests that activity has migrated to the north, as happened before when the Miocene basin became inactive [e.g., *Kashai and Croker*, 1987; *Garfunkel and Ben-Avraham*, 1996]. This raises a number of fundamental questions on the mechanics involved in basin migration, the influence of transverse faults and the displacement history of separate faults.

2.3. Longitudinal Faults

[12] The flat basin floor is bounded on both sides by longitudinal intrabasinal faults named Western and Eastern Intermediate faults in the northern subbasin and Sedom and Ghor Safi faults in the southern subbasin, respectively [e.g., *Neev and Hall*, 1979; *Ben-Avraham et al.*, 1993; *Al-Zoubi et al.*, 2002; *Larsen et al.*, 2002] (Figures 1b and 3). The Western Intermediate Fault (WIF) is the continuation of the Jordan Fault, the main transform fault north of the Dead Sea, and therefore accommodates important strike-slip motion. The southward continuation of the WIF is obscured by the Lisan Diapir, it is therefore unclear whether the WIF and the Sedom Fault are directly linked or not. Along the eastern side, strike-slip motion could be accommodated by the Ghor Safi Fault (GSF) or the Eastern Boundary Fault (EBF), or by both. The strong dip-slip component complicates the recognition and analysis of the strike-slip component on intrabasinal faults. Whether these faults are still active along their entire length at present day, or whether parts of them have become inactive as strike-slip faults with the formation of new transverse faults and the associated basin migration remains unresolved.

[13] The strike-slip motion along the western basin border is considered to occur along the Western Longitudinal Fault in the northern [*Neev and Hall*, 1979], and the Sedom Fault in the southern basin. An intermediate fault block between intrabasinal fault and border fault forms the transition from basin floor to footwall on both sides. The shallow block between the Western Boundary Fault and the Western Intrabasinal Fault is referred to as the median [*Kashai and Croker*, 1987] or intermediate block [*Larsen et al.*, 2002]. This block is covered by a maximum of 3500 m of sediments in the southern basin [*ten Brink and Ben-Avraham*, 1989]. The connection between the Sedom Fault and Western Intrabasinal Fault to the north is unclear, although a ''micro''-pull-apart basin has been observed along the in the continuation of the Western Intrabasinal Fault [*Bartov and Sagy*, 2004]. From detailed fault analyses along the western side of the DSB, *Sagy et al.* [2003] propose that the strike-slip faults form first and that the border normal faults develop in a later stage to accommodate extension.

[14] The eastern shore is formed by the Eastern Boundary Fault, the northward continuation of the Arava Fault. The Eastern Boundary Fault accommodates both strike-slip and large part of the dip-slip offset (Figures 1b and 3). The intrabasinal Ghor Safi Fault separates the basin floor from a small median block [*Al-Zoubi and ten Brink*, 2001].

2.4. Transverse Faults

[15] A number of SE striking transverse faults cross the basin. Many of these faults are only imaged within the basin fill and their presence in the basement could not be proven owing to a lack of deep seismic data. Transverse faults recognized in the basin fill may likely terminate on the evaporites (for depth location, see Figure 3), without affecting the basement. The basin depth increases relatively gradually from the north and the South toward the center

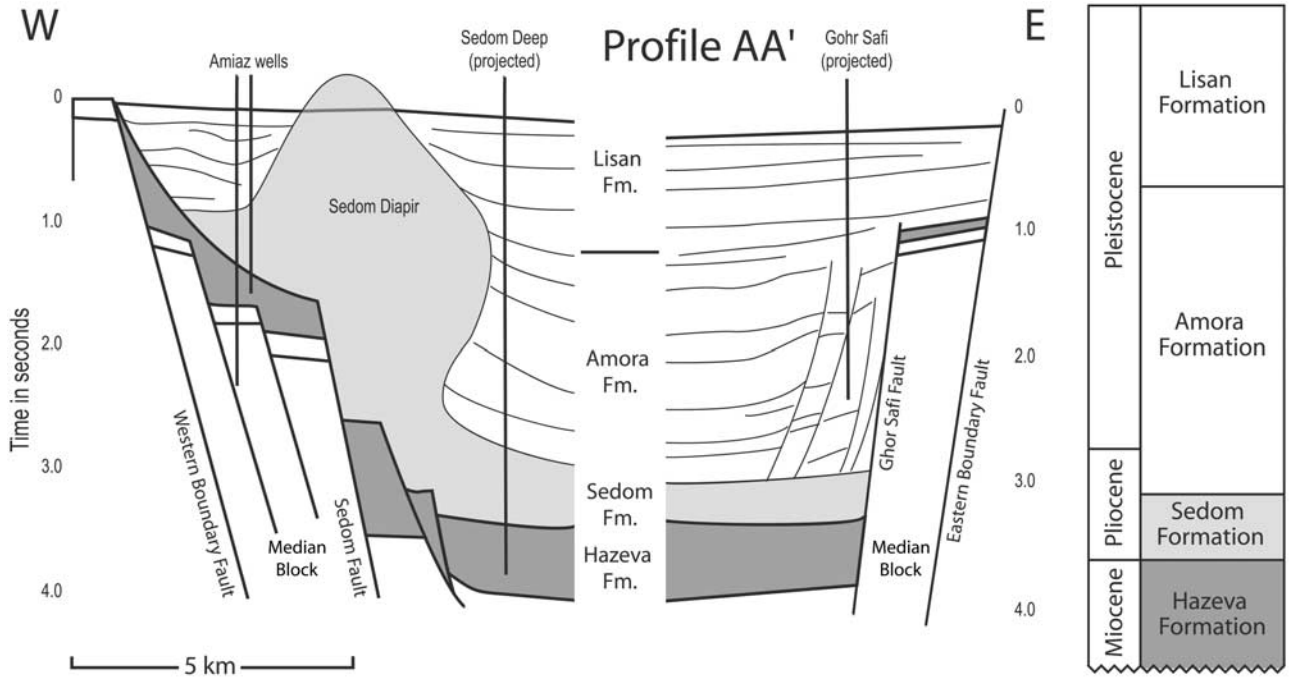

Figure 3. Cross section through southern Dead Sea Basin (modified from data of *Al-Zoubi et al.* [2002]) (see Figure 1 for location).

as can be seen on seismic refraction [*Ginzburg and Ben-Avraham*, 1997] and gravity data (Figure 1b) [*ten Brink and Ben-Avraham*, 1989].

[16] A small number of transverse faults can be traced into the basement, among them the Iddan, Amazyahu and Ein Gedi faults. In the south, the Iddan Fault forms the border between the northern Arava valley and the southern Dead Sea Basin (Figure 1b); this fault is imaged on reflection seismic profiles as a $60°-70°$ northward dipping normal fault that continues into the basement. The Amazyahu Fault, 20 km north of the Iddan Fault, is a NW-SE trending listric normal fault that soles in the evaporites, accommodating ~5.5 km of stretching of the basin fill [e.g., *ten Brink and Ben-Avraham*, 1989]. The analysis of the seismic stratigraphy indicates that activity of the rollover, associated to the listric fault, started in the lower-middle Pleistocene. The 50 m high fault escarpment points to recent slip [*ten Brink and Ben-Avraham*, 1989]. Seismic lines indicate that the basement along the Amazyahu Fault is affected by normal faults [*Kashai and Croker*, 1987; *Larsen et al.*, 2002]. North of the Lisan diapir, the Ein Gedi fault zone corresponds to the edge of the northern basin [*Neev and Hall*, 1979].

[17] Although the northern limit of the DSB appears to be flexural based on gravity analyses (Figure 1b) [e.g., *ten Brink and Ben-Avraham*, 1989; *ten Brink et al.*, 1993], the $M_l = 5.2$ earthquake of February 2004, suggests the presence of a basement transverse fault [*Lazar et al.*, 2006; *Al-Tarazi et al.*, 2006; European Mediterranean Seismological Centre, Earthquake mb 5.1 in Dead Sea region, Jerusalem, 11 Feb. 2004, available at http://www.emsc-csem.org/Html/DEADSEA_110204.html, hereinafter referred to as EMSC, 2004]. The fault plane solution indicates combined dip slip and strike-slip displacement during the main shock (EMSC, 2004) along a northwest-southeast striking fault [*Lazar et al.*, 2006]. Recent studies have shown the prolongation of the basin fill into the Jordan valley where a number of shallow subbasins is separated by transverse faults [e.g., *Lazar et al.*, 2006; *Al-Zoubi et al.*, 2007]. The thick salt layer of the Pliocene Sedom Formation is a complicating factor in the study of the architecture of the Dead Sea Basin. It strongly decouples younger basin fill from the basement and forms a number of large diapiric structures [e.g., *Neev and Hall*, 1979; *Ben-Avraham et al.*, 1993; *ten Brink and Ben-Avraham*, 1989; *Ben-Avraham*, 1997; *Gardosh et al.*, 1997; *Garfunkel*, 1997; *Al-Zoubi and ten Brink*, 2001; *Larsen et al.*, 2002; *Weinberger et al.*, 2006]. Owing to the decoupling of basement from basin fill, structures at the surface and in the basin observed from seismic data cannot necessarily be extrapolated to the basement. Additionally, absorption of seismic energy by the evaporites limits the depth penetration of many seismic lines.

3. Laboratory Experiments

[18] Several experimental modeling studies, both analog [e.g., *Faugère et al.*, 1986; *Jolivet et al.*, 1991; *Dooley and McClay*, 1997; *Rahe et al.*, 1998; *Basile and Brun*, 1999, *Sims et al.*, 1999] and numerical in 2-D [e.g., *Segall and Pollard*, 1980; *Rodgers*, 1980; *Goelke et al.*, 1994] and 3-D [e.g., *Katzman et al.*, 1995; *Petrunin and Sobolev*, 2006] have focused on the structural development of pull-apart basins. Pull-apart basin initiation in laboratory experiments is forced by a lateral step over in the moving basal plate

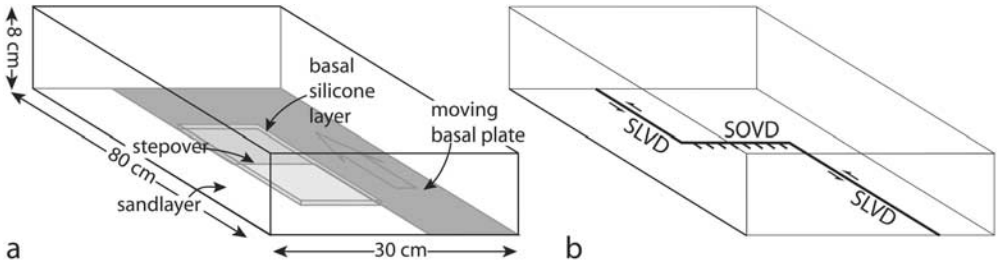

Figure 4. (a) Experimental setup. See text for details. (b) Terminology for basal plate boundary, step over (SOVD) and strike-slip velocity discontinuity, or direction of plate motion (SLVD).

(Figure 4). Different parameters have been experimentally tested, including the width and the angle of the step over and the model's rheology (purely brittle (sand) or brittle/ductile (sand/silicone)). Commonly, the step over width is larger than the thickness of the brittle layer resulting in a pull-apart basin with a long axis that is oblique to the direction of plate motion [e.g., *Rahe et al.*, 1998; *Basile and Brun*, 1999; *Sims et al.*, 1999]. As described in the introduction, the width of the Dead Sea Basin is determined by the between the strike-slip faults, which in case of the Dead Sea Basin is much smaller that that of the crust. It appeared therefore important to test if step overs smaller than model thickness would not be more adapted to the mechanics of Dead Sea-type pull-apart basins. The series of experiments presented in this paper address pull-apart basin geometry and development in terms of fault zone width and crustal rheology.

3.1. Experimental Setup and Procedure

[19] Experiments are carried out using a classical Riedel shear box in which deformation is induced by the displacement of a thin plastic plate at the base of half of the model (Figure 4a). The opposite side of the model is fixed. Pull-apart basins form above a lateral step over velocity discontinuity (SOVD, Figure 4b) in the basal plate that is oriented perpendicular to the direction of plate motion, or strike-slip velocity discontinuity (SLVD, Figure 4b) [e.g., *Jolivet et al.*, 1991; *Dooley and McClay*, 1997; *Basile and Brun*, 1999]. Two widths of the lateral step over in the basal plate (5 and 10 cm), respectively smaller and larger than the model thickness (8 cm) were used. A basal ductile layer representing the ductile crust distributes the applied displacement at a distance from the step over [see also *Jolivet et al.*, 1991; *Basile and Brun*, 1999; *Sims et al.*, 1999]. Two thicknesses of 0.5 and 1.0 cm for this basal ductile layer were tested. Model parameters are summarized in Table 1.

[20] With ongoing basin growth and subsidence, thin sand layers are added to the basin fill at regular time intervals to simulate syntectonic sedimentation. Experiments are presented here by two surface photographs, one before sedimentation and the others in the course of or at the end of deformation. Cross sections are oriented perpendicular to the direction of motion with 2.5 cm spacing.

[21] In the following section we present results of the laboratory experiments for 4 initial set-ups, highlighting the importance of décollement strength and the ratio of step over (fault zone) width to brittle layer thickness.

3.2. Experimental Results

3.2.1. Model 1 (Purely Brittle, Large Step Over)

[22] Deformation starts in the center of the model above the step over with the initiation of two dominantly strike-slip faults (F_1 and F_2), close to Riedel shears in pure strike-slip displacement, that grow outward and accommodate strike-slip and dip-slip motions (Figure 5) thus forming a pull-apart basin. With ongoing motion, the main strike-slip movement is transferred to newly formed intrabasinal faults (F_3 and F_4) that are oriented less oblique to the SLVD (Figure 5). Normal faulting is partly transferred to these newly formed strike-slip faults and partly continued along the border faults. The final basin has a strongly sigmoidal geometry that can be attributed to the absence of a basal ductile décollement level. The wide step over plays a strong role, inducing highly oblique and strongly curved faults. Accordingly, the long axis of the basin strikes at a significant angle to the SLVD. This type of pull-apart basins that forms above a wide basement step over in the absence of a basal décollement is well known from literature [e.g., *Faugère et al.*, 1986; *Dooley and McClay*, 1997].

3.2.2. Model 2 (Thin Basal Décollement, Large Step Over)

[23] The two dominantly strike-slip faults (F_1 and F_2) that initiate above the large step over are less curved and oblique than in model 1. Similar to the previous model, strike-slip and normal faulting concentrates on these initial faults during early stages of basin formation. The largest strike-slip displacements are located along fault F_1 that is less oblique to the SLVD than fault F_2 (Figure 6). With increasing displacement, a new strike-slip fault (F_3) appears in the

Table 1. Model Parameters[a]

	Model			
	1	2	3	4
Step over width (cm)	10.0	10.0	5.0	5.0
Thickness basal silicone (cm)	x	0.5	0.5	1.0

[a]Step over width ($W_{step\ over}$); length × width of the basal silicone layer ($L_{bs} \times W_{bs}$) and the thickness of the basal silicone layer (Z_{bs}).

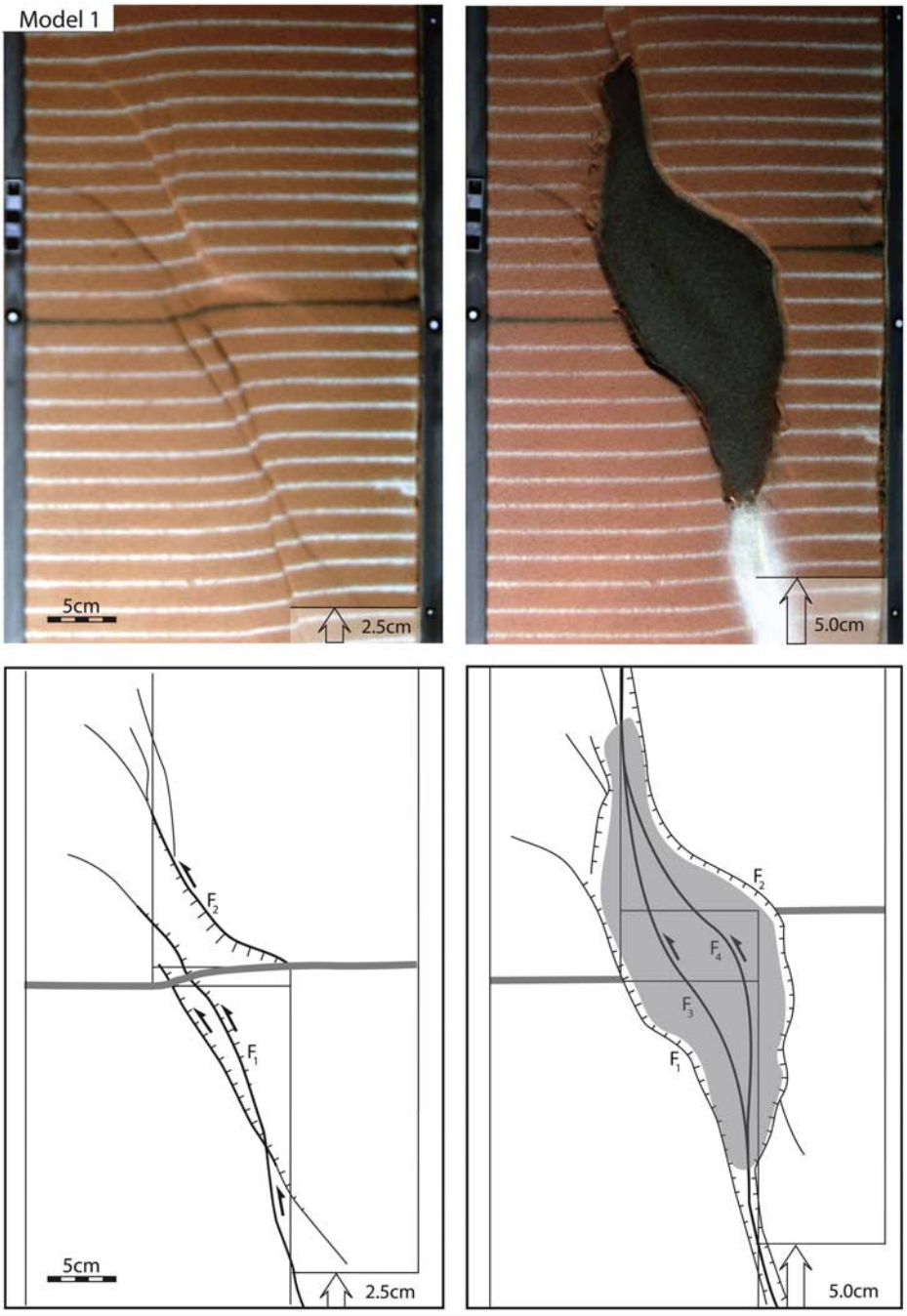

Figure 5. Photos and line drawings of model 1 with a basement step over width of 10 cm, without basal ductile layer. Note that the final basin has a strongly sigmoidal geometry due to the absence of a basal ductile décollement level.

basin center. Fault F_2 is too oblique to accommodate further strike-slip motion but remains active as a normal fault.

[24] During late motion, when the fault pattern is stabilized, a new oblique normal fault (F_4) appears (Figure 6). The pull-apart basin itself, as it is defined by the longitudinal strike-slip faults, forms a subbasin within the initial and larger one that is defined by normal faults highly oblique to the direction of motion. The pull-apart subbasin has a regular elongated shape that trends with a 15° obliquity to the direction of motion. With increasing displacement, transverse normal faults develop outside the basin to accommodate the large extension. Serial cross sections, cut perpendicular to the direction of motion, show that much of the subsidence is accommodated along the boundary normal faults and the intrabasinal strike-slip faults, especially along the western basin side (Figure 7).

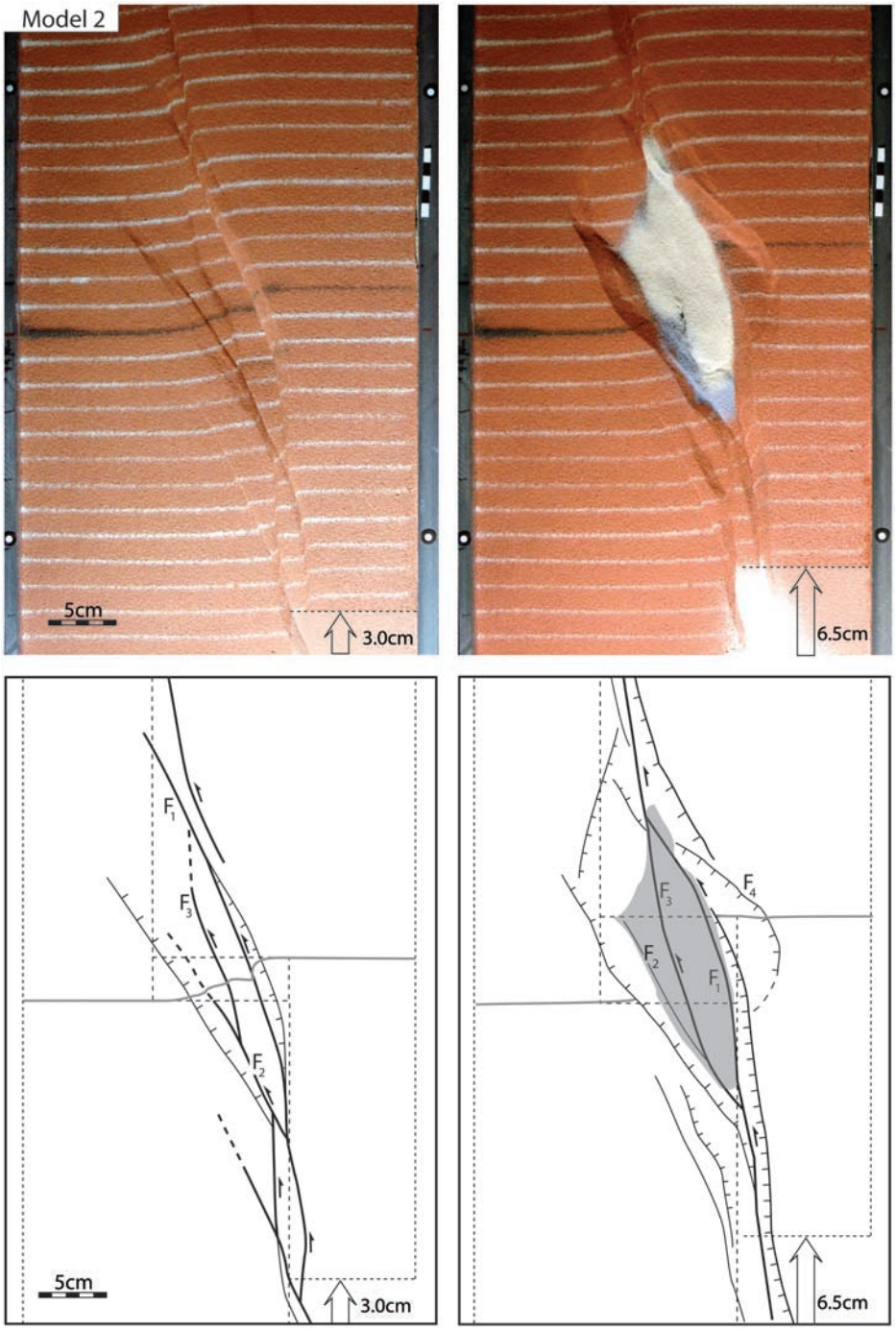

Figure 6. Photos and line drawings of model 2. Setup is same as model 1, apart from the addition of a 5 mm thick basal ductile layer of located above the step over. Dark shading on drawing indicates outline of synkinematic sedimentation; light shading represents total subsided area. The initially wide basin narrows with the initiation of a longitudinal fault within the basin. After 5 cm displacement, highly oblique normal faults develop outside the basin.

[25] Note that in cross sections (Figure 7) all faults have dips, steeper than common for normal faults, i.e., in excess of 60°. The same observation also holds for the following models.

3.2.3. Model 3 (Thin Basal Décollement, Small Step Over)

[26] Owing to the smaller step over, the initial dominantly strike-slip faults (F_1 and F_2) are less oblique to the direction

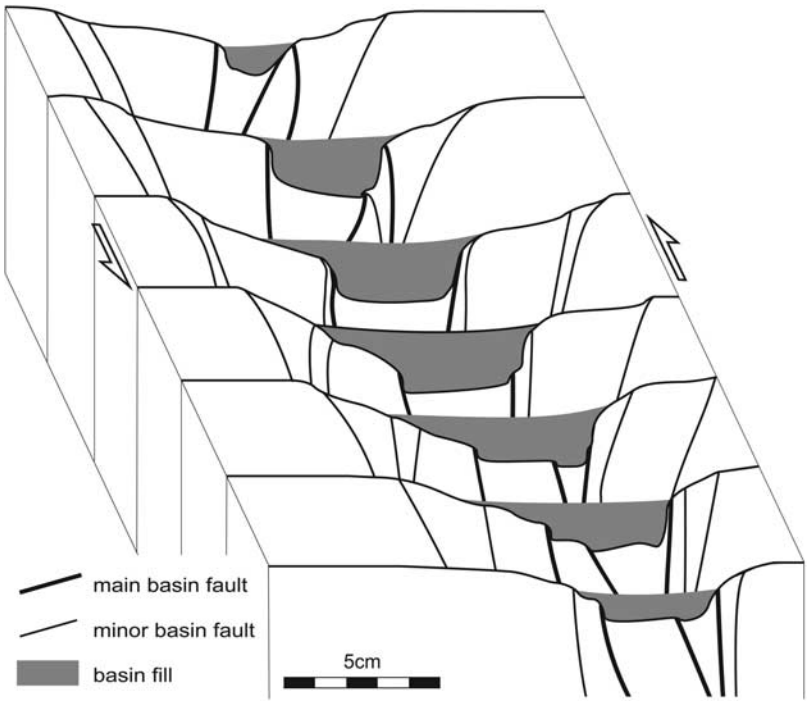

Figure 7. Cross sections of model 2. Most of the subsidence is accommodated along the border and intrabasinal faults, especially along the western side. The pull-apart basin, as defined by the strike-slip faults, occupies less than half the width of the total basin.

of motion and more regularly distributed along the fault zone than in previous models (Figure 8). These initial faults are very close to Riedel shears, regularly spaced and oriented at 15° to the direction of motion. These faults define the short sides of the basin. The long sides are defined by a new strike-slip fault (F_3) and by propagation of F_1 toward fault F_2. The geometry and orientation of the inner part of the basin as defined by the latest strike-slip faults are similar to that of the pull-apart basin in the previous model. At a late stage, a NW-SE trending transverse fault (F_4) appears in the southern part of the basin that cuts both basement and basin fill (Figure 8). As a result, the active depocenter migrates in the motion direction and basin subsidence stops on the other side of F_4. Owing to the small basement step over deformation and subsidence are distributed along a large part of the fault zone resulting in a shallower basin with a basin floor that deepens to the north (Figure 9). Cross sections confirm that the limited subsidence is almost fully concentrated on the strike-slip faults.

3.2.4. Model 4 (Thick Basal Décollement, Small Step Over)

[27] The early faults are shorter and more closely spaced than in previous models. A number of them remain active as strike-slip faults and interconnect to form the southern and western basin border faults (F_1) (Figure 10). The eastern border is formed by a fault (F_2) that propagates southward in the nondeformed area, east of the early faults. The northern edge of the basin is flexural during most of the deformation. As a whole, the basin is elongated and regularly shaped with a flat floor bordered by two parallel N-S trending strike-slip faults (F_1 and F_2).

[28] Subsidence is regularly distributed over the length of the long and narrow basin and therefore rather slow compared to the other models and accommodated along the border strike-slip faults (Figure 11). Although surface views give little indication for their presence, cross sections show that additional border normal faults do form finally; defining small intermediate blocks (Figure 11). Near the southern edge of the basin, a NW-SE transverse fault (F_3) initiates in late stages to form the new southern border of the basin. A second NW-SE trending transverse fault (F_4) appears along the, northern rim of the basin that until then was flexural (Figure 10). Together, the two transverse faults decrease the basin length and cause an inward depocenter migration.

4. Discussion of Experimental Results

[29] The experiments demonstrate that basins forming in the absence of a basal ductile layer are characterized by a sigmoidal geometry in surface view (Figure 5) [see also *Faugère et al.*, 1986].

[30] Decreasing the width of the step over strongly decreases the amount and rate of subsidence. The comparison between model 2 (Figure 6) and model 3 (Figure 8) shows that the actual pull-apart basins are quite similar. At the same time, the highly oblique and partly sigmoidal normal faults that accommodate the strong subsidence in model 2 are absent in model 3. In the latter case the step

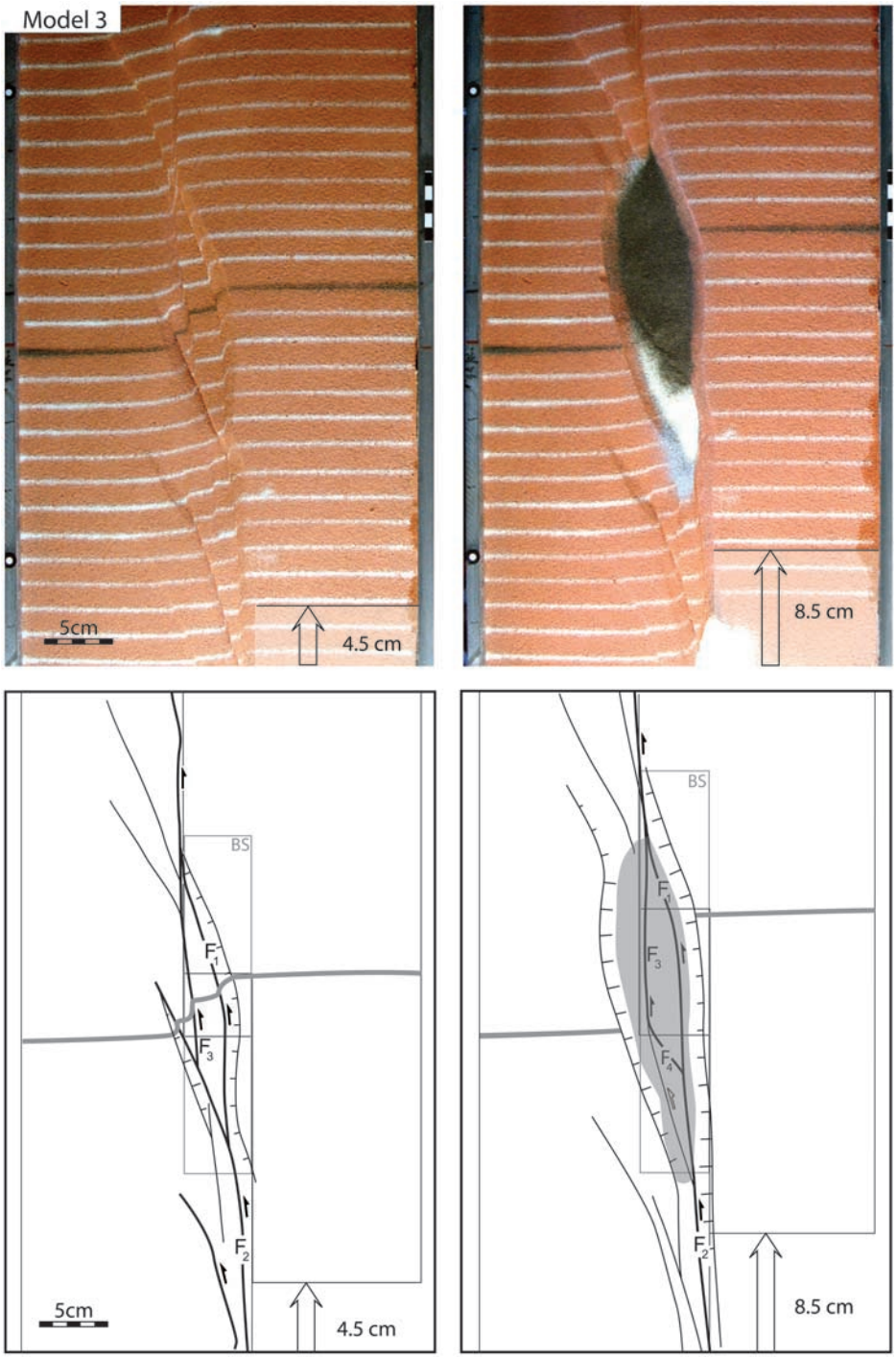

Figure 8. Photos and line drawings of model 3 with the same setup as model 2, except the small basement step over of 5.0 cm. The basin's regular shape is defined by the initial faults. The white sand on the right photograph outlines the part of the basin that became inactive with basin migration and is partly covered with dark sand in the remaining active part. Pale shading on drawings shows that subsidence is almost fully concentrated in the basin.

over width is smaller than the thickness of the brittle layer.

[31] Pull-apart basins that develop above a small step over (i.e., smaller than the model thickness) have a reduced width and become more rectangular and more parallel to the overall motion. These effects increase with an increasing decoupling along the basal ductile layer. In the experiment with the largest degree of decoupling along the basal ductile

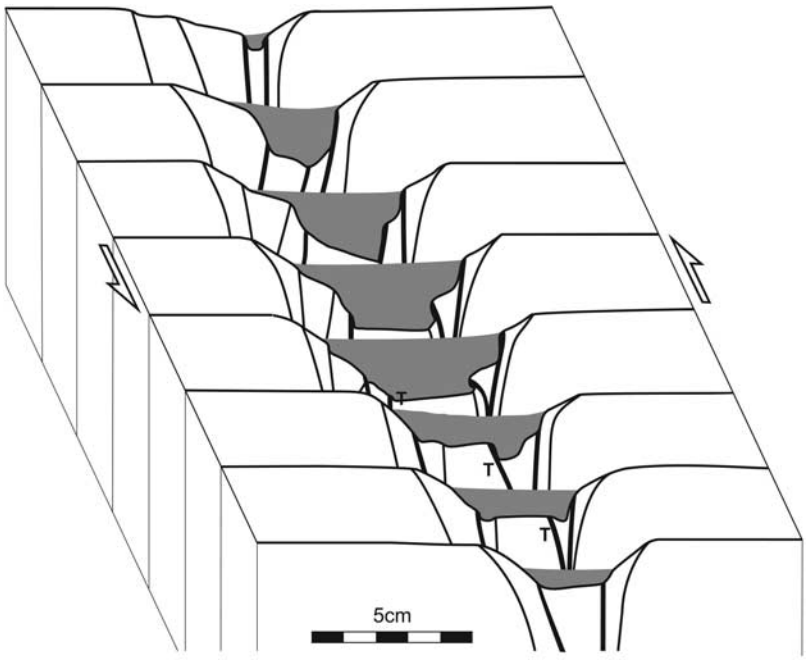

Figure 9. Cross sections of model 3. T indicates late transverse fault responsible for basin migration. Note the limited basin depth south of the transverse fault.

layer, the basin has a nearly rectangular geometry, is elongated parallel to the strike-slip basal boundary (Figure 10) and has a flat basin floor (Figure 11).

[32] Longitudinal strike-slip faults border the basin floor over its entire length. Their steep to vertical dip implies that the distance between them remains constant. Consequently, the pull-apart basin itself does not widen with ongoing deformation. During a first stage, basin subsidence is accommodated along these strike-slip faults. Then, normal faults without strike-slip component form at the rim of the basin to accommodate extension that results from the oblique orientation of the basin with respect to the imposed displacement.

[33] Three types of transverse faults are identified in the models. The first one is a basin border fault, it is present in basins whose north and south margins are bordered by faults since the onset of deformation (e.g., F_1 and F_2 in model 1, Figure 5). These transverse faults are the remnants of incipient Riedel-like faults. The second type of transverse faults occurs in basins with initially or gradually subsiding, extremities (i.e., no fault). With ongoing subsidence, when the subsidence gradient becomes too strong to be accommodated solely by flexure, transverse faults initiate to accommodate further subsidence (e.g., F_4 in model 3, Figure 8). The third type, the intrabasinal faults, is related to basin migration (e.g., F_4 in model 4, Figure 10). When the transverse fault connects the two border strike-slip faults, the displacement is transferred from the southern part of the eastern fault to the northern part of the western fault. Consequently, the southern part of the basin becomes inactive and subsidence concentrates in the northern part.

[34] In a pure strike-slip setting, the basin's longitudinal strike-slip faults are parallel to the regional displacement field. In the absence of a regional transtensional component, the amount of extension on border faults oriented normal to the fault zone depends on the angle between basin and direction of movement and the width of the basement step over. This implies that, if the fault zone is not transtensional at a regional scale, basins that are elongated parallel to the direction of plate movement will show little or no extension perpendicular to their elongation, nevertheless the strong dip-slip component of faults.

5. Comparison of Experimental Results and the Dead Sea Basin

[35] The ratio between crustal thickness and amount of displacement is a critical parameter in scaling length between model and prototype. The amount of displacement applied to the DSB is poorly known owing to uncertainties in the exact age of the oldest sediments, i.e., Miocene clastics of the Hazeva Formation [e.g., *Garfunkel*, 1997]. However, these 2 km thick sediments must be of pre-Pliocene age. Accordingly, the DSB accommodated at least 40 km of plate motion, which is more than its crustal thickness. Since the total displacement applied to the experiments does not exceed the model thickness, the final length and architecture cannot be compared to the full complexity of the present-day Dead Sea Basin. However, in view of this limitation, it is remarkable how well experimental results, in particular model 4, fit to the architecture of the present DSB (Figure 12).

[36] Experimental results give insight into a number of features related to Dead Sea-type elongated pull-apart basins, including the appearance of intrabasinal transverse faults and basin migration.

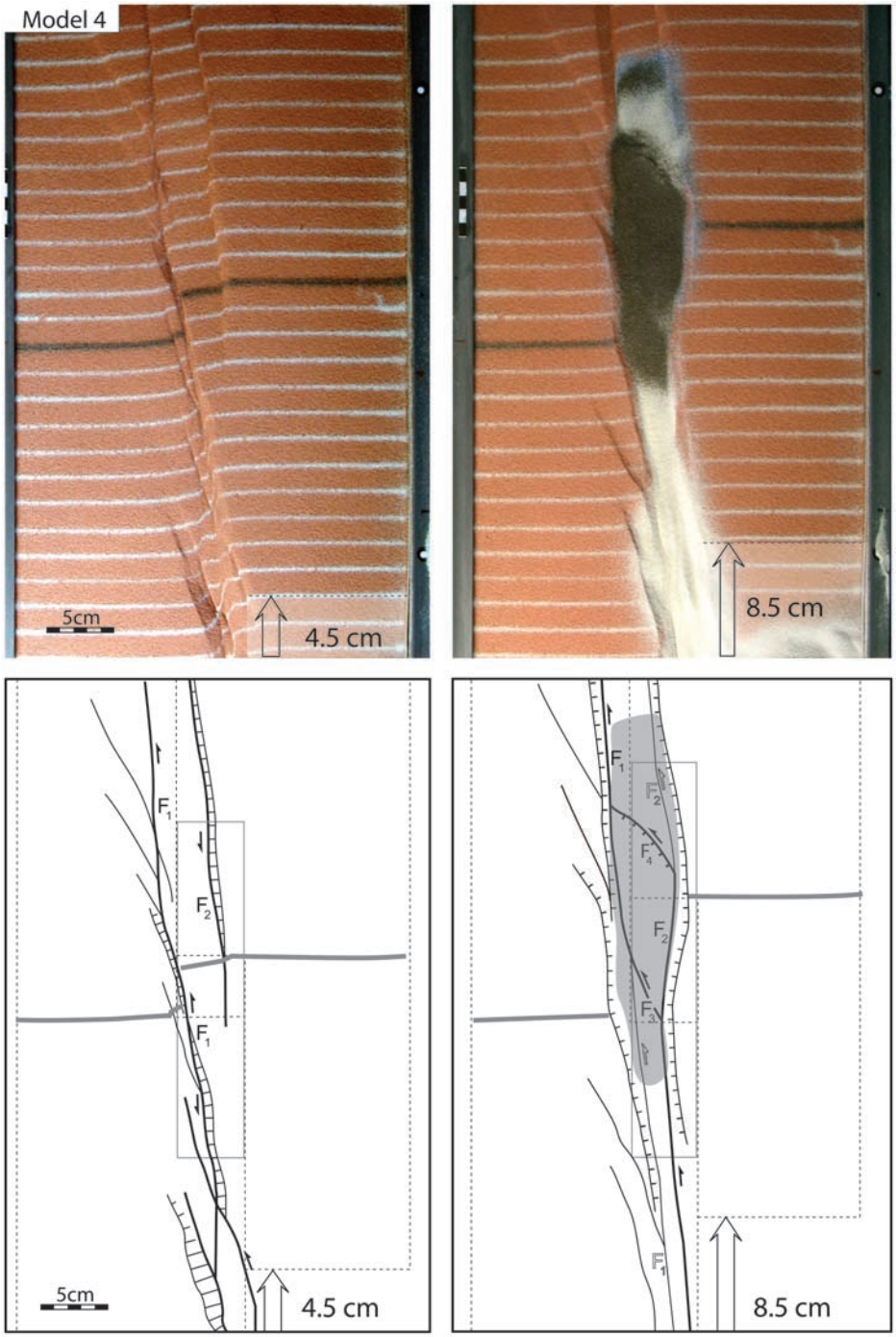

Figure 10. Photos and line drawings of model 4. Experimental setup is as in model 3 but with a twice as thick basal ductile layer (1.0 cm). The initial basin is defined by subsidence between two parallel longitudinal faults. Northern and southern borders are flexural. Figure 10 (right) shows late transverse faults that are responsible for the inward migration of the depocenter.

5.1. Death Valley Versus Dead Sea

[37] The relatively small distance between the fault segments along the DSF leads to rather elongated and nearly rectangular basins with long axis parallel to the bounding strike-slip faults (Figure 2a). Experiments show that in fault zone-parallel pull-apart basins, the longitudinal strike-slip faults define the basin geometry and that basin extremities may be flexural instead of being defined by faults. This is in strong contrast to Death Valley type pull-apart basins (Figure 2b) that are highly oblique to the transform direction, with transverse normal faults dominating over longi-

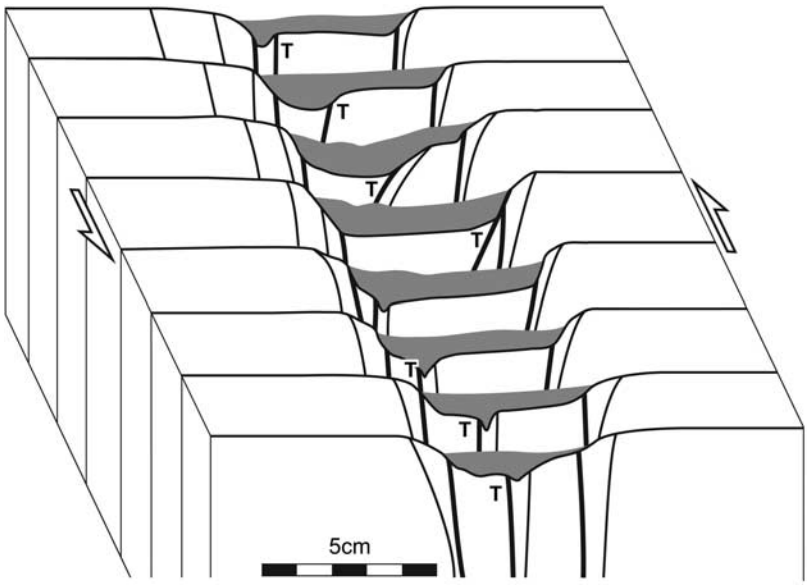

Figure 11. Cross sections of model 4. T indicates late transverse fault responsible for basin migration. The basin floor is remarkably flat, whereas offset on border normal faults is small.

tudinal strike-slip faults. The architecture of these oblique basins is closer to an oblique rift than to transform parallel basins, like those along the DSF. It follows that the ratio of fault zone or corridor width, with respect to crustal thickness is an important parameter in the mechanics of pull-apart basin formation within transform corridors like the Dead Sea Fault.

5.2. Strike-Slip Faulting

[38] Recognition of a strike-slip component on a fault is often difficult and in pull-apart basins further complicated by the strong dip-slip component on the faults. Strike-slip faults border the flat basin floor on both sides along the full basin length. In basins bordered by both normal and strike-slip faults, the faults bordering the flat basin floor have a strike-slip component. For the Dead Sea, these are the Sedom and Western Intrabasinal faults along the western side and the Ghor Safi Fault and its northern continuation along the eastern side of the basin (Figure 12a).

5.3. Normal Faulting

[39] The presented experimental results show a dominant role of pure normal faults at the basin rims to accommodate basin subsidence when the basin trends oblique to the motion direction. Normal faults become increasingly important with increasing basin obliquity. In the models with the highest obliquity (models 1 and 2), border normal faults are dominant and determine the basin's outline. On the contrary, the basin is almost parallel to the motion direction in model 4 and as a result border normal faults are of minor importance (Figure 12b). This confirms that the normal faults observed along the DSB's borders may result from a slight local or regional transtension [e.g., *Quennell*, 1958, 1959; *Garfunkel*, 1981; *Ben-Avraham and Zoback*, 1992].

5.4. Intrabasinal Transverse Faults and Basin Migration

[40] Because the evaporites decouple the younger basin fill from the basement, the transverse faults in the Pliocene to Recent basin fill do not necessarily reflect the presence of basement faults. Transverse faults are linked to basin migration in the experimental models (Figures 8, 10 and 12b). With the initiation of a transverse fault, activity of the western transverse fault ceases south of it, resulting in northward basin migration (Figure 12). In other words, when transverse fault are linked to basin migration, the occurrence of the latter provides an indication for the presence of these faults. In the Dead Sea Basin, basin migration seems to have occurred twice: first when the Miocene segment in the Arava Valley became inactive and, second, when basin subsidence switched from the Southern Dead Sea to the Northern Basin, reflected in the contrast in bathymetry, varying from subaerial to a 300 m water depth, respectively. The first migration can probably be linked to the Iddan Fault that is known from seismic data to be a basement fault. Recognition of the fault related to the second migration is complicated by the thick salt layer that decouples the young sediments from basement and the lack of resolution of seismic lines below the salt. The Ein Gedi Fault [*Neev and Hall*, 1979] may have played a key role in the second basin migration. This would also imply that the Amazyahu basement fault, imaged on seismic data, has a different origin and that it possibly accommodates north-south stretching of the basement.

[41] Whereas in experiments transverse faults are oriented more or less parallel to σ_1, at 30°–45° with respect to displacement direction, transverse faults are usually drawn perpendicular to the displacement direction (see Figure 12

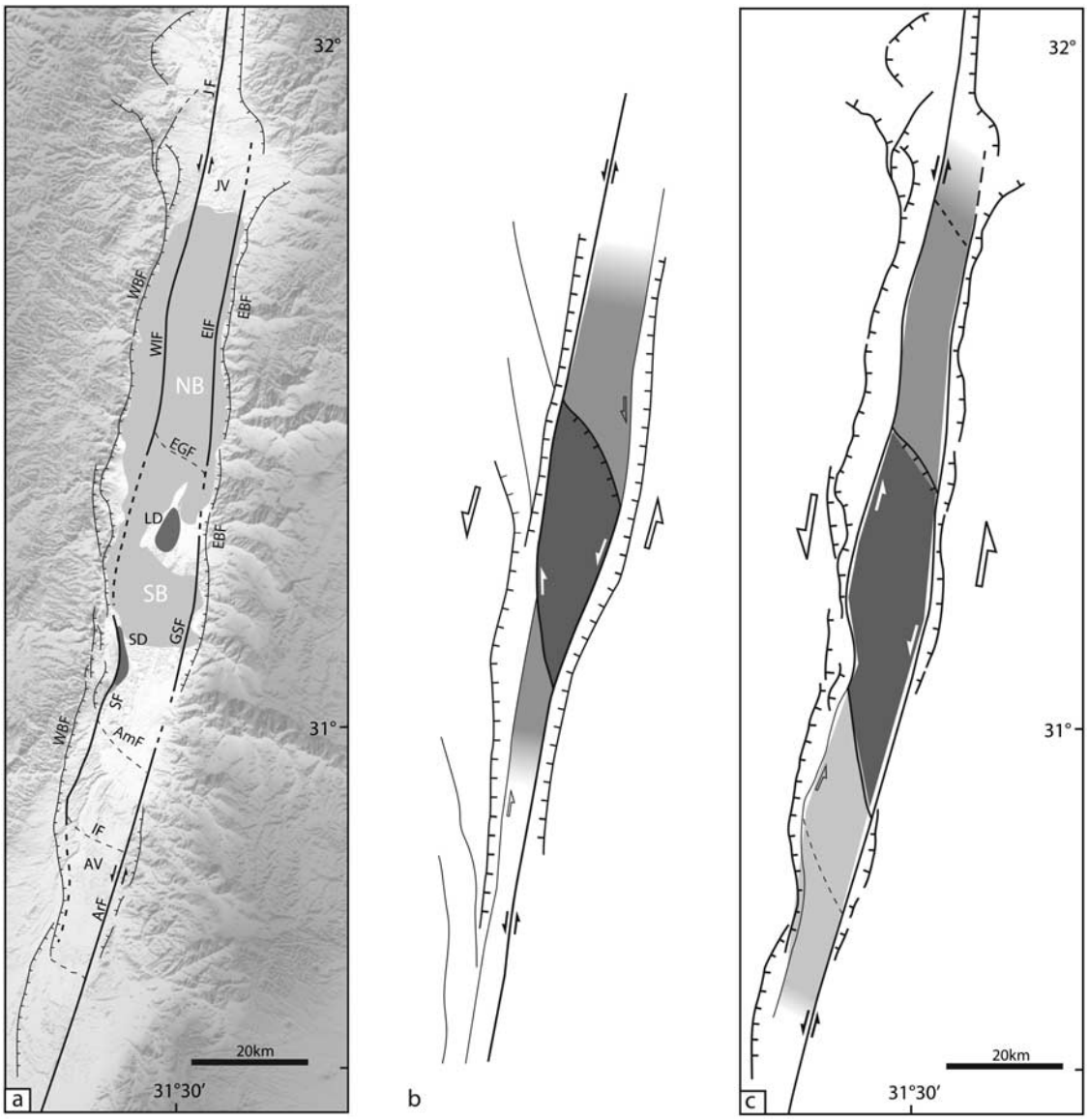

Figure 12. Interpretation of the architecture of the Dead Sea Basin based on experimental results. a) Digital elevation model of the central segment of the Dead Sea Fault with the location of main structural features controlling the geometry of the Dead Sea Basin. b) Basin configuration of laboratory experiment most closely to the DSF in terms of initial experimental setup (model 4). c) Structural interpretation of the DSB inferred from comparison of basin geometry and fault patterns (Figure 12a) with the results from laboratory experiment model 4 (Figure 12b), showing that the compartmentalization of the DSB in different subbasins, with pronounced differences in geometry is largely controlled by temporal and spatial basin migration. Extrapolation of experimental results to the Dead Sea suggests that transverse faults are oriented NW-SE instead of east-west.

for comparison). This discrepancy may be due to the limited data concerning exact position and orientation of these faults in the Dead Sea.

5.5. Northern Basin Margin: Gradual or Transverse Fault

[42] The gradual deepening of the basin from the north toward the basin center and the associated minor normal faulting along its southern and northern border suggest gradual, flexure-like deepening along the northern and southern Dead Sea margins, compatible with model 4 (Figure 12) and the model based on gravity modeling proposed by *ten Brink and Ben Avraham* [1989]. As in model 4, transverse faults may have initiated in later stages to accommodate subsidence after the gradients became too steep. This might explain the recent M_l = 5.2 May 2004

earthquake at the northern rim of the DSB [*Lazar*, 2004; *Al-Tarazi et al.*, 2006].

5.6. Step Over Width and Rheology

[43] The ratio between step over width and thickness of the deforming layer determines not only the basin width but its geometry and its development as well. Basins that develop above a wide step over have a long axis trending at high angles to the direction of motion, an irregular geometry and important normal faulting. The regular and nearly rectangular shape of the DSB is due to the small width of the transform zone.

[44] The comparison between model 3 (Figures 8 and 9) and model 4 (Figures 10 and 11) shows the importance of decoupling along the lower ductile crust. For both models, basal step over width and displacement rate are identical, but in model 4 the ductile layer is twice as thick. Consequently, the ductile strength in model 4 is half that of model 3, and the decoupling between the upper brittle layer (crust) and the basal plates (mantle) is twice as effective in model 4. This results in a more elongated, regular shape and symmetrical basin geometry in model 4. This supports the existence of a high degree of decoupling between upper crust and uppermost mantle along the lower ductile crust along the Dead Sea Basin, (Figure 12), which is in general agreement with results from numerical modeling [*Petrunin and Sobolev*, 2006]. This contradicts an almost brittle lower crust, a conclusion based on the observed deep seismicity in the DSB [*Aldersons et al.*, 2003; *Shamir*, 2006]. Alternative mechanisms for DSB formation that consider a fully brittle crust, like drop down basin (DDB) discussed by *Ben-Avraham and Schubert* [2006], have not been tested in the present study.

6. Conclusions

[45] Contrary to other examples, Dead Sea-type pull-apart basins form within the rather narrow transform corridor between strike-slip faults that are less than 10 km apart, much smaller than the crustal thickness of 35 km. Until now, experimental studies have mostly concentrated on the development of much wider pull-apart basins including the influence of a basal ductile layer representing the lower ductile crust. This paper has concentrated on the consequences of fault zone width and rheology for the mechanics of pull-apart basin formation. Pull-apart basins that develop above a small step over (i.e., smaller than model thickness) are reduced in width and are more rectangular and more parallel to the overall motion. The partly sigmoidal, highly oblique, normal faults that accommodate the strong subsidence are absent in models with a step over width smaller than model thickness. The presence of a basal ductile layer results in a more regular fault pattern and a pull-apart basin that is less oblique to the direction of motion. These effects increase with increasing decoupling along the basal ductile layer. In the experiment with the strongest mechanical decoupling, the orthorhombic basin is almost parallel to the strike-slip basal boundary and as a result, normal faulting is minor. The short extremities are flexures until new transverse faults form to accommodate further subsidence. The flat basin floor is bordered by two straight faults over its full length. Basin migration takes place after the initiation of a new intrabasinal transverse fault. Comparison between the model and the DSB yields that normal faulting especially along the eastern border of the DSB is likely the result of regional transtension and not of the pull-apart basin itself. The flat basin floor of the DSB is bordered over its full length by strike-slip faults. The elongated and regularly orthorhombic basins with long axes parallel to the bounding strike-slip faults appear to be controlled by the relatively small distance between the strike-slip fault segments. Experiments show that the longitudinal strike-slip faults define the basin geometry as well as basin migration in DSF-type pull-apart basins and that basin extremities may be flexural instead of being defined by faults. This is in strong contrast to Death Valley type pull-apart basins that are highly oblique to the transform direction with transverse normal faults dominating over longitudinal strike-slip faults. The architecture of these oblique basins is closer to an oblique rift than that of transform parallel basins like the basins along the DSF. It follows that the ratio of basin width and crustal thickness as well as the lithosphere rheology are controlling factors in the mechanics of pull-apart basin formation within transform corridors such as the Dead Sea Fault System.

[46] **Acknowledgments.** The experiments presented in this paper have been performed in the experimental tectonics laboratory of Géosciences Rennes as part of the first author's Ph.D. thesis, jointly granted by Vrije Universiteit Amsterdam and the Université de Rennes 1 [*Smit*, 2005]. We thank J.-J. Kermarrec for his help in setting up the experiments. Remarks from two anonymous reviewers helped to improve the manuscript. J.S. acknowledges financial support from the Netherlands Research Centre for Integrated Solid Earth Sciences (ISES) and a Marie Curie Fellowship in the framework of the European Doctoral Training Centre for Sedimentary Basin Studies (Eurobasins). J.P.B. acknowledges financial support from the Institut Universitaire de France. Suggestions and comments by the two anonymous reviewers were greatly appreciated.

References

Al-Tarazi, E., E. Sandvol, and F. Gomez (2006), The February 11, 2004 Dead Sea earthquake ML = 5.2 in Jordan and its tectonic implication, *Tectonophysics*, *422*, 149–158, doi:10.1016/j.tecto.2006.05.010.

Al-Zoubi, A., and U. ten Brink (2001), Salt diapirs in the Dead Sea Basin and their relationship to Quaternary extensional tectonics, *Mar. Pet. Geol.*, *18*, 779–797, doi:10.1016/S0264-8172(01)00031-9.

Al-Zoubi, A., H. Shulman, and Z. Ben-Avraham (2002), Seismic reflection profiles across the southern Dead Sea Basin, *Tectonophysics*, *346*, 61–69, doi:10.1016/S0040-1951(01)00228-1.

Al-Zoubi, A. S., T. Heinrichs, I. Qabbani, and U. S. ten Brink (2007), The northern end of the Dead Sea Basin: Geometry from reflection seismic evidence, *Tectonophysics*, *434*, 55–69, doi:10.1016/j.tecto.2007.02.007.

Aldersons, F., Z. Ben-Avraham, A. Hofstetter, E. Kissling, and T. Al-Yazjeen (2003), Lower-crustal strength under the Dead Sea Basin from local earthquake data and rheological modeling, *Earth Planet. Sci. Lett.*, *214*, 129–142, doi:10.1016/S0012-821X(03)00381-9.

Aydin, A., and A. Nur (1982), Evolution of pull-apart basins and their scale independence, *Tectonics*, *1*, 91–105, doi:10.1029/TC001i001p00091.

Aydin, A., and A. Nur (1985), The types and role of stepovers in strike-slip tectonics, in *Strike-Slip Deformation, Basin Formation, and Sedimentation*, edited by K. T. Biddle and N. Christie-Blick, *SEPM Spec. Publ.*, *37*, 35–44.

Bartov, Y., and A. Sagy (2004), Late Pleistocene extension and strike-slip in the Dead Sea Basin, *Geol. Mag.*, *141*, 565–572, doi:10.1017/S001675680400963X.

Basile, C., and P. Allemand (2002), Erosion and flexural uplift along transform faults, *Geophys. J. Int.*, *151*, 646–653, doi:10.1046/j.1365-246X.2002.01805.x.

Basile, C., and J. P. Brun (1999), Transtensional faulting patterns ranging from pull-apart basins to transform continental margins; an experimental investigation, *J. Struct. Geol.*, *21*, 23–37, doi:10.1016/S0191-8141(98)00094-7.

Ben-Avraham, Z. (1985), Structural framework of the Gulf of Elat (Aqaba), northern Red Sea, *J. Geophys. Res.*, *90*, 703–726, doi:10.1029/JB090iB01p00703.

Ben-Avraham, Z. (1997), Geophysical framework of the Dead Sea, in *The Dead Sea: The Lake and Its Settings*, edited by T. M. Niemi, Z. Ben-Avraham, and J. Gat, pp. 22–35, Oxford Univ. Press, New York.

Ben-Avraham, Z., and G. Schubert (2006), Deep "drop down" basin in the southern Dead Sea, *Earth Planet. Sci. Lett.*, *251*, 254–263, doi:10.1016/j.epsl.2006.09.008.

Ben-Avraham, Z., and M. D. Zoback (1992), Transform-normal extension and asymmetric basins; an alternative to pull-apart models, *Geology*, *20*, 423–426, doi:10.1130/0091-7613(1992)020<0423:TNEAAB>2.3.CO;2.

Ben-Avraham, Z., T. M. Niemi, D. Neev, J. K. Hall, and Y. Levy (1993), Distribution of Holocene sediments and neotectonics in the deep north basin of the Dead Sea, *Mar. Geol.*, *113*, 219–231, doi:10.1016/0025-3227(93)90019-R.

Blakely, R. J., R. C. Jachens, J. P. Calzia, and V. E. Langenheim (1999), Cenozoic basins of the Death Valley extended terrane as reflected in regional-scale gravity anomalies, in *Cenozoic Basins of the Death Valley Region*, edited by L. A. Wright and B. W. Troxel *Spec. Pap., Geol. Soc. Am.*, *333*, 1–16.

Bosworth, W., P. Huchon, and K. McClay (2005), The Red Sea and Gulf of Aden basins, *J. Afr. Earth Sci.*, *43*, 334–378, doi:10.1016/j.jafrearsci.2005.07.020.

Burchfiel, B. C., and J. H. Stewart (1966), 'Pull-apart' origin of the central segment of Death Valley, California, *Geol. Soc. Am. Bull.*, *77*, 439–441, doi:10.1130/0016-7606(1966)77[439:POOTCS]2.0.CO;2.

Christie-Blick, N., and K. T. Biddle (1985), Deformation and basin formation along strike-slip faults, in *Strike-Slip Deformation, Basin Formation, and Sedimentation*, edited by K. T. Biddle and N. Christie-Blick, *SEPM Spec. Publ.*, *37*, 1–34.

Chu, D., and R. G. Gordon (1998), Current plate motions across the Red Sea, *Geophys. J. Int.*, *135*, 313–328, doi:10.1046/j.1365-246X.1998.00658.x.

Cloetingh, S., and Z. Ben-Avraham (Eds.) (2002), *From Extension to Collision: The Dead Sea Rift and Other Natural Laboratories, Stephan Mueller Spec. Publ. Ser.*, 246 pp., Eur. Geosci. Union, Strasbourg, France.

Crowell, J. C., (1974), Origin of late Cenozoic basins in southern California, in *Tectonics and Sedimentation*., edited by W. R. Dickinson, *SEPM Spec. Publ.*, *37*, 190–204.

DESERT Group et al. (2004), The crustal structure of the Dead Sea Transform, *Geophys. J. Int.*, *156*, 655–681, doi:10.1111/j.1365-246X.2004.02143.x.

Dooley, T., and K. McClay (1997), Analog modeling of pull-apart basins, *AAPG Bull.*, *81*, 1804–1826.

Enzel, Y., A. Agnon, and M. Stein (Eds.) (2006), *New Frontiers in Dead Sea Paleoenvironmental Research*, *Spec. Pap. Geol. Soc. Am.*, 253 pp.

Faugère, E., J. P. Brun, and J. van den Driessche (1986), Bassins asymetriques en extension pure et en decrochement; modeles experimentaux, *Bull. Cent. Rech. Explor. Prod. Elf Aquitaine*, *10*, 13–21.

Gardosh, M., E. Kashai, S. Salhov, H. Shulman, and E. Tannenbaum (1997), Hydrocarbon exploration in the southern Dead Sea area, in *The Dead Sea: The Lake and Its Setting*, edited by T. M. Niemi, Z. Ben-Avraham, and J. R. Gat, pp. 57–72, Oxford Univ. Press, Oxford, U.K.

Garfunkel, Z. (1981), Internal structure of the Dead Sea leaky transform (rift) in relation to plate kinematics, *Tectonophysics*, *80*, 81–108, doi:10.1016/0040-1951(81)90143-8.

Garfunkel, Z. (1997), The history and formation of the Dead Sea Basin, in *The Dead Sea: The Lake and Its Settings*, edited by T. M. Niemi, Z. Ben-Avraham, and J. Gat, pp. 36–56, Oxford Univ. Press, New York.

Garfunkel, Z., and Z. Ben-Avraham (1996), The structure of the Dead Sea Basin, *Tectonophysics*, *266*, 155–176, doi:10.1016/S0040-1951(96)00188-6.

Garfunkel, Z., and Z. Ben-Avraham (2001), Basins along the Dead Sea Transform, in *Peri-Tethyan Rift/Wrench Basins and Passive Margins*, *Peri-Tethys Mem.*, vol. 6, edited by P. A. Ziegler et al., pp. 607–627, Mus. Natl. d'Hist. Nat., Paris.

Ginzburg, A., and Z. Ben-Avraham (1997), A seismic refraction study of the northern basin of the Dead Sea, Israel, *Geophys. Res. Lett.*, *24*, 2063–2066, doi:10.1029/97GL01884.

Ginzburg, A., J. Makris, K. Fuchs, and C. Prodehl (1981), The structure of the crust and upper mantle in the Dead Sea Rift, *Tectonophysics*, *80*, 109–119, doi:10.1016/0040-1951(81)90144-X.

Goelke, M., S. Cloetingh, and K. Fuchs (1994), Finite-element modelling of pull-apart basin formation, *Tectonophysics*, *240*, 45–57, doi:10.1016/0040-1951(94)90263-1.

Hurwitz, S., Z. Garfunkel, Y. Ben-Gai, M. Reznikov, Y. Rotstein, and H. Gvirtzman (2002), The tectonic framework of a complex pull-apart basin: seismic reflection observations in the Sea of Galilee, Dead Sea transform, *Tectonophysics*, *359*, 289–306, doi:10.1016/S0040-1951(02)00516-4.

Izzeldin, A. Y. (1987), Seismic, gravity and magnetic surveys in the central part of the Red Sea; their interpretation and implications for the structure and evolution of the Red Sea, *Tectonophysics*, *143*, 269–306, doi:10.1016/0040-1951(87)90214-9.

Joffe, S., and Z. Garfunkel (1987), Plate kinematics of the circum Red Sea: A re-evaluation, *Tectonophysics*, *141*, 5–22, doi:10.1016/0040-1951(87)90171-5.

Jolivet, L., P. Huchon, J.-P. Brun, X. Le Pichon, N. Chamot-Rooke, and J.-C. Thomas (1991), Arc deformation and marginal basin opening: Japan Sea as a case study, *J. Geophys. Res.*, *96*, 4367–4384, doi:10.1029/90JB02455.

Kashai, E. L., and P. F. Croker (1987), Structural geometry and evolution of the Dead Sea-Jordan rift system as deduced from new subsurface data, *Tectonophysics*, *141*, 33–35, doi:10.1016/0040-1951(87)90173-9.

Katzman, R., U. S. ten Brink, and J. Lin (1995), Three-dimensional modeling of pull-apart basins; implications for the tectonics of the Dead Sea Basin, *J. Geophys. Res.*, *100*, 6295–6312, doi:10.1029/94JB03101.

Kocyigit, A., A. Yilmaz, S. Adamia, and S. Kuloshvili (2001), Neotectonics of east Anatolian Plateau (Turkey) and Lesser Caucasus: Implication for transition from thrusting to strike-slip faulting, *Geodin. Acta*, *14*, 177–195, doi:10.1016/S0985-3111(00)01064-0.

Larsen, B. D., Z. Ben-Avraham, and H. Shulman (2002), Fault and salt tectonics in the southern Dead Sea Basin, *Tectonophysics*, *346*, 71–90, doi:10.1016/S0040-1951(01)00229-3.

Lazar, M. (2004), Tectonic processes along the northern edges of pull-apart basins in the Dead Sea rift: A case study from the northern Dead Sea, Ph.D. thesis, 140 pp., Tel Aviv Univ., Tel Aviv, Israel.

Lazar, M., Z. Ben-Avraham, and U. Schattner (2006), Formation of sequential basins along a strike-slip fault—Geophysical observations from the Dead Sea Basin, *Tectonophysics*, *421*, 53–69, doi:10.1016/j.tecto.2006.04.007.

Le Pichon, X., and J. M. Gaulier (1988), The rotation of Arabia and the Levant fault system, *Tectonophysics*, *153*, 271–294, doi:10.1016/0040-1951(88)90020-0.

McKenzie, D. P., D. Davies, and P. Molnar (1970), Plate tectonics of the Red Sea and east Africa, *Nature*, *226*, 243–248, doi:10.1038/226243a0.

Mohsen, A., R. Kind, S. V. Sobolev, M. Weber, and Desert Group (2006), Thickness of the lithosphere east of the Dead Sea Transform, *Geophys. J. Int.*, *167*, 845–852, doi:10.1111/j.1365-246X.2006.03185.x.

Neev, D., and J. K. Hall (1979), Geophysical investigations in the Dead Sea, *Sediment. Geol.*, *23*, 209–238, doi:10.1016/0037-0738(79)90015-0.

Niemi, T. M., Z. Ben-Avraham, and J. Gat (Eds.) (1997), *The Dead Sea: The Lake and Its Settings*, 298 pp., Oxford Univ. Press, New York.

Petrunin, A., and S. V. Sobolev (2006), What controls thickness of sediments and lithospheric deformation at a pull-apart basin?, *Geology*, *34*, 389–392, doi:10.1130/G22158.1.

Quennell, A. M. (1958), The structural and geomorphic evolution of the Dead Sea rift, *Q. J. Geol. Soc. London*, *114*, 1–24.

Quennell, A. M. (1959), Tectonics of the Dead Sea rift, paper presented at the 20th International Geological Congress, Assoc. de Serv. Geol. Afr., Mexico City, Mexico.

Rahe, B., D. A. Ferrill, and A. P. Morris (1998), Physical analog modeling of pull-apart basin evolution, *Tectonophysics*, *285*, 21–40, doi:10.1016/S0040-1951(97)00193-5.

Reilinger, R., et al. (2006), GPS constraints on continental deformation in the Africa-Arabia-Eurasia continental collision zone and implications for the dynamics of plate interactions, *J. Geophys. Res.*, *111*, B05411, doi:10.1029/2005JB004051.

Rodgers, D. A. (1980), Analysis of pull-apart basin development produced by en echelon strike-slip faults, in *Sedimentation in Oblique-Slip Mobile Zones*, edited by P. F. Balance and H. G. Reading, *Spec. Publ. Int. Assoc. Sediment.*, *4*, 27–41.

Ruppert, S., M. M. Fliedner, and G. Zandt (1998), Thin crust and active upper mantle beneath the southern Sierra Nevada in the western United States, *Tectonophysics*, *286*, 237–252, doi:10.1016/S0040-1951(97)00268-0.

Sagy, A., Z. Reches, and A. Agnon (2003), Hierarchic three-dimensional structure and slip partitioning in the western Dead Sea pull-apart, *Tectonics*, *22*(1), 1004, doi:10.1029/2001TC001323.

Segall, P., and D. D. Pollard (1980), Mechanics of discontinuous faults, *J. Geophys. Res.*, *85*, 4337–4350, doi:10.1029/JB085iB08p04337.

Sengör, A. M. C., N. Görür, and F. Saroglu (1985), Strike-slip faulting and related basin formation in zones of tectonic escape; Turkey as a case study, in *Strike-Slip Deformation, Basin Formation, and Sedimentation*, edited by K. T. Biddle and N. Christie-Blick, *SEPM Spec. Publ.*, *37*, 227–264.

Shamir, G. (2006), The active structure of the Dead Sea Depression, in *New Frontiers in Dead Sea Paleoenvironmental Research*, edited by Y. Enzel, A. Agnon, and M. Stein, *Spec. Pap. Geol. Soc. Am.*, *401*, 15–32.

Sims, D., D. A. Ferrill, and J. A. Stamatakos (1999), Role of a ductile decollement in the development of pull-apart basins: Experimental results and natural examples, *J. Struct. Geol.*, *21*, 533–554, doi:10.1016/S0191-8141(99)00010-3.

Smit, J. (2005), Brittle-ductile coupling in thrust wedges and continental transforms, Ph.D. thesis, 115 pp, Vrije Univ., Amsterdam.

Sylvester, A. G. (1988), Strike-slip faults, *Geol. Soc. Am. Bull.*, *100*, 1666–1703, doi:10.1130/0016-7606(1988)100<1666:SSF>2.3.CO;2.

ten Brink, U. S., and Z. Ben-Avraham (1989), The anatomy of a pull-apart basin; seismic reflection observations of the Dead Sea Basin, *Tectonics*, *8*, 333–350, doi:10.1029/TC008i002p00333.

ten Brink, U. S., Z. Ben-Avraham, R. E. Bell, M. Hassouneh, D. F. Coleman, G. Andreasen, G. Tibor, and B. J. Coakley (1993), Structure of the Dead Sea pull-apart basin from gravity analyses, *J. Geophys. Res.*, *98*, 21,877–21,894.

ten Brink, U. S., M. Rybakov, A. S. Al-Zoubi, M. Hassouneh, U. Frieslander, A. T. Batayneh, V. Goldschmidt, M. N. Daoud, Y. Rotstein, and J. K. Hall (1999), Anatomy of the Dead Sea Transform; does it reflect continuous changes in plate motion?, *Geology*, *27*, 887–890, doi:10.1130/0091-7613(1999)027<0887:AOTDST>2.3.CO;2.

Wakabayashi, J., J. V. Hengesh, and T. L. Sawyer (2004), Four-dimensional transform fault processes: progressive evolution of step-overs and bends, *Tectonophysics*, *392*, 279–301, doi:10.1016/j.tecto.2004.04.013.

Wdowinski, S., and E. Zilberman (1997), Systematic analyses of the large-scale topography and structure across the Dead Sea Rift, *Tectonics*, *16*, 409–424, doi:10.1029/97TC00814.

Weinberger, R., Z. B. Begin, N. Waldmann, M. Gardosh, G. Baer, A. Frumkin, and S. Wdowinski (2006), Quaternary rise of the Sedom Diapir, Dead Sea Basin, in *New Frontiers in Dead Sea Paleoenvironmental Research*, edited by Y. Enzel, A. Agnon, and M. Stein, *Spec. Pap. Geol. Soc. Am.*, *401*, 33–51.

Wright, L. A., , and B. W. Troxel (Eds.) (1999), *Cenozoic Basins of the Death Valley Region*, *Spec. Pap. Geol. Soc. Am.*, *333*, 392 pp.

Zak, I., and R. Freund (1981), Asymmetry and basin migration in the Dead Sea Rift, *Tectonophysics*, *80*, 27–38, doi:10.1016/0040-1951(81)90140-2.

Z. Ben-Avraham, Department of Geophysics and Planetary Sciences, Tel Aviv University, Tel Aviv 69978, Israel.

J.-P. Brun, Géosciences Rennes, UMR 6118, Université de Rennes 1, Campus de Beaulieu, CNRS, Bâtiment 15, F-35042 Rennes CEDEX, France.

S. Cloetingh, Netherlands Research Centre for Integrated Solid Earth Sciences, Faculty of Earth and Life Sciences, Vrije Universiteit, De Boelelaan 1085, NL-1081 HV Amsterdam, Netherlands.

J. Smit, Department of Earth Sciences, ETH Zurich, Leonhardstrasse, 19/LEB, CH-8092 Zürich, Switzerland. (jeroen.smit@erdw.ethz.ch)